Available online at www.CivileJournal.org

Civil Engineering Journal

(E-ISSN: 2476-3055; ISSN: 2676-6957)

Vol. 11, No. 07, July, 2025

A Novel One-Sided Push-Out Test for Shear Connectors in Composite Beams

Luay M. Shather [1], M. A. Hussein Al-Shuwaili [1*]

[1] *Faculty of Engineering, University of Kufa, Najaf, 54001, Iraq.*

Received 22 February 2025; Revised 19 June 2025; Accepted 24 June 2025; Published 01 July 2025

Abstract

The small-scale push-out test (POT) is widely utilized to investigate the characteristic behavior of shear connectors as an available alternative to full-scale beam tests, which are often costly and time-consuming. However, several researchers have expressed issues regarding the POT specimen setup during testing due to inconsistencies between the results of POTs and beam bending tests. In this paper, a new configuration for a one-slab POT is developed to address these issues. To validate the developed method of testing, several POTs and OSPOTs were conducted and compared against each other and with those of previous research. The load-slip curves obtained from the OSPOTs were then evaluated against the curves obtained from four empirical expressions. Furthermore, a database of different POT configurations and setups, specifically 114 tests, selected from the previous research that employed the 19 mm shear stud, was analyzed in detail. Subsequently, the results of these tests and the proposed OSPOT method were compared with the predictions offered by several empirical equations. The results indicated that the results of the OSPOT are more consistent with the codes and empirical equations compared to typical POT. Hence, this OSPOT setup could be used as an efficient and economic option for the POT, as it has the potential to double the number of results for the same resources and simplify the casting procedure, which is particularly significant when numerous tests are required for the experimental campaign. Also, the OSPOT results revealed more ductile behavior for the shear studs, which is consistent with the full-scale beams' testing.

Keywords: Composite Beams; Shear Studs; Push-Out Test (POT); One-Sided Push-Out Test (OSPOT); Load-Slip Curve.

1. Introduction

Composite concrete slabs and steel beams effectively combine the best properties of both materials, offering less deflection, a higher span-to-depth ratio, and cost-effectiveness [1]. Shear studs, i.e., headed studs, commonly interconnect the slabs to beams, facilitating the shear transmission between the two elements and subsequently defining the structural performance of the composite beams. Hence, the accurate characterization of the shear studs is significant. This characterization is expressed through the relationship between the applied load (P) and the relative displacement at the steel-concrete interface, known as slip (δ). The significance of the P-δ curve is that it reveals the shear resistance, ductility, and stiffness of the investigated shear connectors [2]. The P-δ relationship should be found from full-scale beam testing to simulate the performance of the shear connectors in the actual medium, i.e., a large concrete slab.

The full-scale testing presents several challenges: (i) the full-scale testing (FST) is time-consuming and complicated (ii) the flexural forces in the composite beam create indirect loading for the connectors which complicates the evaluation of the shear transfer mechanism between concrete and steel; (iii) the variety of connection methods makes it unattainable to determine the ductility and strength of shear connectors from composite beam tests [3]. In addition, Oehlers &

* Corresponding author: mohammed.abdulhussein@uokufa.edu.iq

http://dx.doi.org/10.28991/CEJ-2025-011-07-05

Bradford (1995) [3] emphasized that "composite beam tests are expensive, and this would prohibit the development of shear connectors". Consequently, the POT method has been introduced as a viable alternative to the full-scale beam testing More recently POTs employed by Gyawali et al. (2024) [4] and Yu et al. (2025) [5].

In the traditional POT, two identical reinforced concrete blocks (slabs) are attached to a steel section, usually an ɪ-shaped, by means of the investigated shear connectors A direct longitudinal shear force is applied to the steel section through hydraulic jack The P-δ curve in the POT is usually plotted to represent the relationship between the relative longitudinal movement at the concrete-steel interface (in the direction of the load) and the applied load.

Although Push-out tests may not fully replicate the actual behavior and conditions, the performance POT offers a practical approach for examining shear connectors in composite beams due to several key factors: (i) the size of the POT specimen and its economy compared to FSTs; ii) investigating under the direct shear loading offers a clear view about the performance of shear connector [6] ; iii) a variety of parameters can be investigated and the characteristic behavior of shear connectors can be evidenced; iv) The comparative analysis of various types sizes and geometries of shear connectors can be effectively conducted; v) it is possible to measure the relative displacement between the steel profile and the concrete slabs in both directions, vertically and horizontally, i.e. slip and separation, during the test. vi) The relationship between applied load and resulting stresses in the concrete, rebars, and shear connectors can be obtained directly, and this relationship is notably simpler than in the case of FST, as it solely relates to shear stresses [7].

Since the 1930s, researchers have widely used numerous POTs specimens to evaluate the resistance of shear connectors [8]. However, due to the POT setup, many researchers have indicated inconsistencies between POT and FST results. Oehlers & Bradford (1995) [3] and Hicks & McConnel (1997) [9], among the other researchers, believe that the conventional setup of the POT increases the connectors' shear resistance due to the induced frictional forces at the base of the specimen, thus influencing the measured shear resistance. Consequently, the Load-slip (P-δ) relation resulting from a POT is highly influenced by the boundary conditions of the concrete slab [10, 11].

Other authors also aimed to reduce or eliminate the frictional reaction by using various POT setups wherein the base of the specimen is either free to slide in both directions or restricted in the horizontal direction, as shown in Figure 1. Nevertheless, the confinement might affect the quantified shear resistance of the connectors. Applying a horizontal restraint equal to 10% of the applied testing force can lead to a 14% increase in shear resistance [12]. Also in this content, Lorenc et al. (2010) [13] presented a modified disposition for POT testing attempting to stimulate the behavior of the composite beam under the sagging moment conditions. It is worth mentioning that Eurocode-4 (2005) (EC-4) [14] recommends embedding the sample base in mortar or gypsum, while BS 5400-5 (2005) (BS-5) [15] suggests providing a hard base to support the slabs of the specimen.

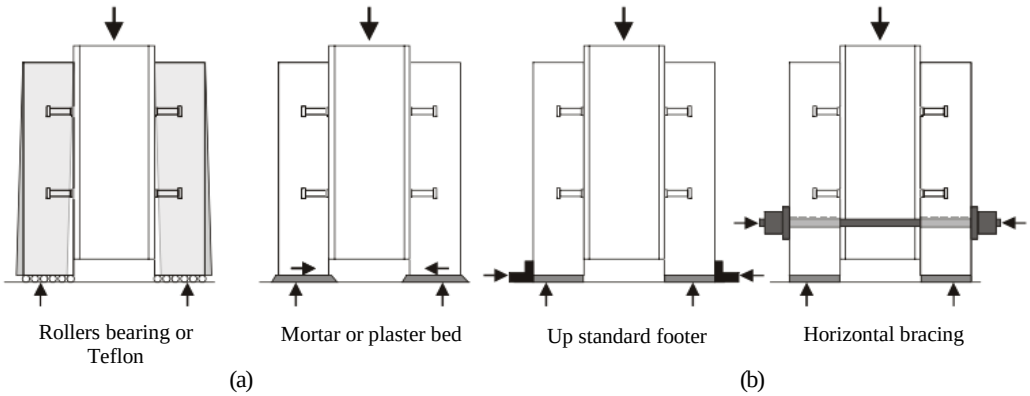

Figure 1. Different POT setups (a) free to slide and (b) restricted to slide [16]

1.1. One-Slab Push-out Test (OSPOT)

The variation in the specimen's size and setup is intended to minimize the discrepancy between the FCS and POT results caused by the frictional reaction under the base of the specimen. To pursue this aim, several researchers have developed one-slab POT (OSPOT) specimens, which can be tested in either vertical or horizontal positions and classified as horizontal and vertical OSPOT. Various researchers have employed the OSPOT method and have not shown any significant impact on the behavior of the shear connectors [17].

Ernst (2006) [17] indicated that the OSPOT, used by Patrick (2000) [18] and Hicks & McConnel (1997) [9], had no significant impact on shear connector behavior. Lam (2000) [19], Zaki et al. (2003) [20], Topkaya et al. (2004) [21] and Jayas & Hosain (2010) [22] utilized a horizontal OSPOT. Ghiami Azad (2016) [23] reviewed the horizontal OSPOT conducted by other researchers. More recently, Lowe et al. (2014) [24], Suwaed et al. (2022) [25] Li et al. (2023) [26] and Ding et al. (2024) [27] employed similar horizontal setups. Ernst (2006) [17], Valente (2007) [7] and Classen & Gallwoszus (2016)[28], among other researchers, employed the vertical OSPOT.

However, OSPOT with sliding bearings may underestimate the actual shear resistance of the connector. Notably, the horizontal OSPOT, requires some significant changes to the testing frame, and in many cases, these changes can only accommodate specific specimens and connectors. This paper presents a developed one slab POT configuration that addresses the shortcomings of previous POT and OSPOT setups. A key feature of the developed OSPOT is its ability to acquire two results from a standard POT specimen, effectively doubling the output for the same resources and reducing the time spent in the testing campaigns.

2. New One-Slab Push-Out Test (OSPOT)

Ernst (2006) [17] identified inconsistencies in the results obtained from the vertical OSPOT apparatus, see Figure 2-a, when subjected to high-loading conditions, particularly with test specimens featuring multiple-headed studs. The application of eccentric high loading led to a separation between the spreader loading beam and the specimens, resulting in increased horizontal movement at the upper section of the specimen. This separation increased the horizontal movement of the specimen at the top part of the specimen as the vertical RHS tube steel behaves similarly to a cantilever column (see Figure 2-b).

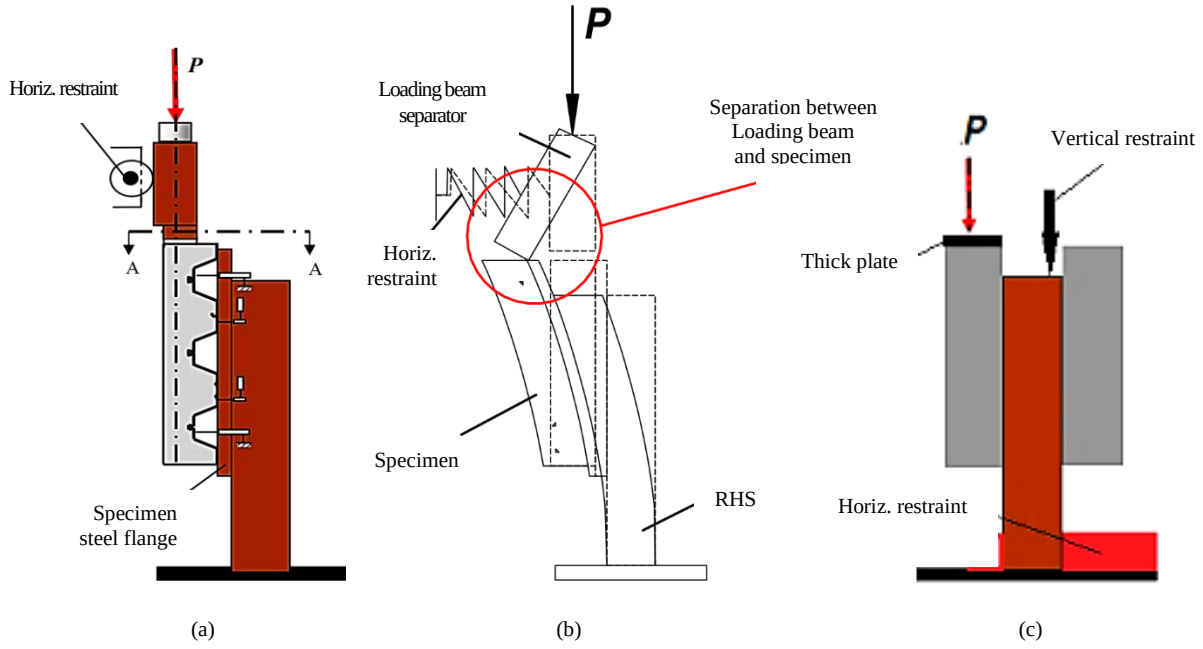

Figure 2. (a) OSPOT by Ernst [17] (b) setup shortcoming [17] and (c) design concepts of the developed OSPOT setup [29]

To enhance the reliability and accuracy of the vertical OSPOT, several modifications are implemented, as shown in Figure 2-c, to address the shortcomings observed in Ernst's (2006) [17] setup and also eliminate the frictional reaction as the slap is free to move in the load direction as shown in Figure 2-c [29]:

- Removal of the Load Spreader Beam: The new setup subjects a direct load to the concrete slab through a thick plate, ensuring uniform load distribution across the specimen. This adjustment eliminates the separation between the loading plate and the slab, thereby preventing any horizontal movement during testing.
- Vertical Restraint Implementation: A vertical restraint is added at the upper section of the steel beam. This involves integrating a bracing steel beam parallel to the slabs, providing enhanced stability to the specimen and preventing any forward lean during testing. This modification effectively addresses the eccentricity of the applied shear load in relation to the reaction at the base of the steel beam.
- Addition of Secondary Horizontal Restraint: A secondary horizontal restraint is introduced at the base of the steel beam to further strengthen the stability during the testing process see Figure 3.
- Utilisation of Traditional POT Specimens: To ensure greater stability during the casting and preparation phases, a traditional POT is employed, i.e. two concrete slabs attached to I-steel section using headed studs. In this modified OSPOT setup, the specimen is supported by the steel section while the load is applied sequentially to each slab, see Figure 3, allowing for movement in the direction of the load application.

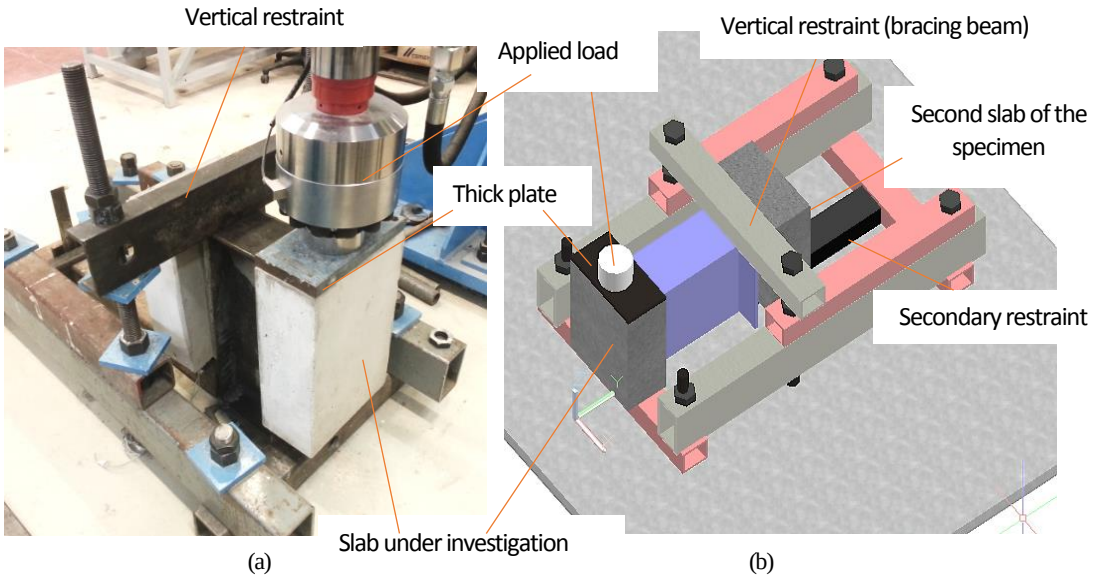

Figure 3. OSPOT setup and fasten the vertical restraint (bracing beam) and the secondary restraint [29]

This approach facilitates the gathering of two distinct results from a single POT specimen and not one result as normally happen.

These enhancements are aimed at improving the precision and reliability of the OSPOT testing methodology, ultimately contributing to a deeper understanding of the shear connector's behaviors being investigated.

2.1. Typical POT vs. Developed OSPOT

While the OSPOT and POT specimens are similar, as shown Figure 4, the new OSPOT setup effectively removes the frictional force by permitting the slab to move freely in the direction of the load, as OSPOT specimen is directly supported by the steel section. In contrast, the POT configuration rests on the concrete slabs and the steel section moves in the load direction. Additionally, in the OSPOT arrangement, the stud resists both the applied load and the weight of the slab, which is similar to full-scale beam testing.

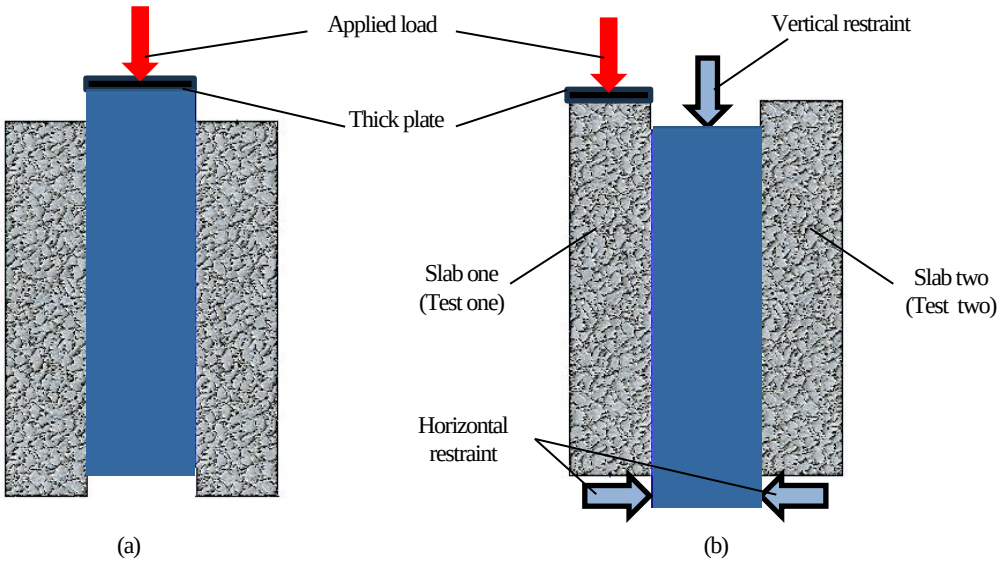

Figure 4. (a) Typical push-out test (POT), (b) developed one slab POT

In the POTs, normally, the weaker of the two concrete slabs fails prior to the other side [7, 17]. Consequently, the POT results are the average performance of two slabs, i.e. one result from two slabs. While in the OSPOT method, only one slab is tested at a time, avoiding the unnecessary duplication of slabs, which leads to a signification reduction in labour, cost and time.

3. Experimental Program

Figure 5 shows the methodology used to achieve the aim of this research.

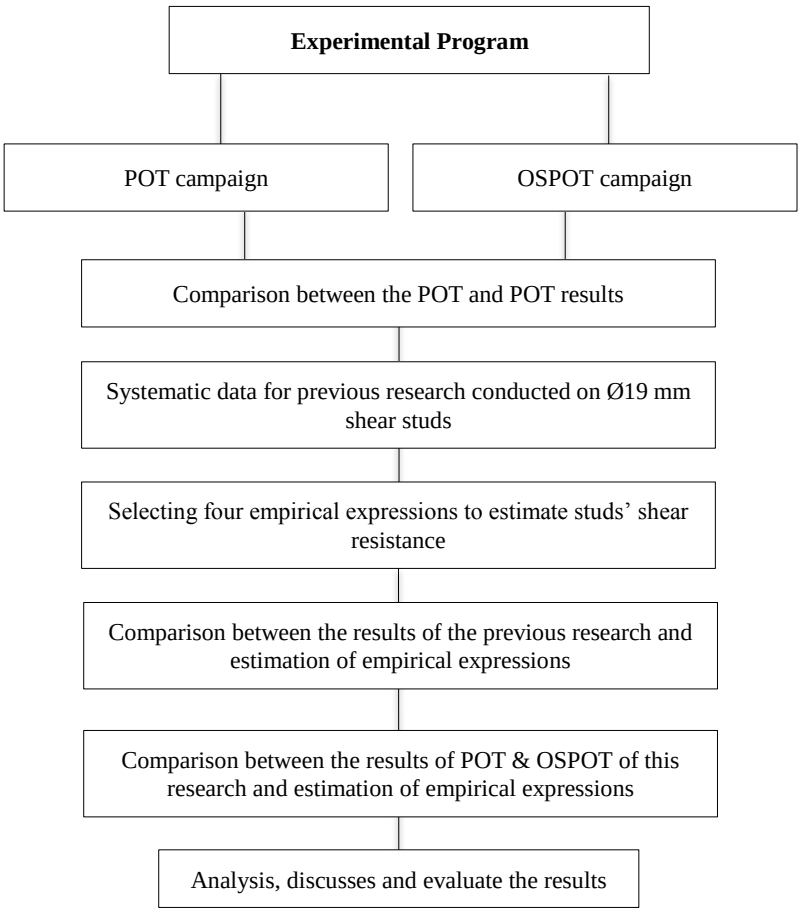

Figure 5. Research methodology flowchart

3.1. Layout of Test Specimen

The most widely used headed studs are 19 mm in diameter and 100 mm in height with a 450 N/mm tensile strength [30]; hence, 19 mm studs were used in this testing campaign. The fabrication of specimens adhered to the specifications of the standard POT recommended by BS 5400-5:2005 [14]. Each specimen utilized two shear studs, 19 × 80 mm, one on each side, except for the final test, which incorporated two studs on each side. The headed studs were welded directly to a British Universal Beam (UB) 254 × 146 × 43 mm (with a depth of 260 mm, a width of 147 mm, and a weight of 43 kg/m), measuring 560 mm in length. To ensure a uniform distribution of any axial load applied to the beam, two 12 mm thick steel plates were also welded to the top and bottom ends of the steel beam. The studs bond two concrete slabs, of 460 × 300 × 150 mm (height × width × thickness) each, to the greased flanges of the steel section (see Figure 6).

All the slabs of the specimens were reinforced with two Ø10 transverse stirrups, except two specimens, as shown in Figure 6. The first stirrup and a 19 mm stud were positioned 70 mm and 225 mm, respectively, from the top surface of the concrete, which was subject to the applied load. The clear distance between the upper and lower stirrups was 250 mm.

The OS-Ø8-17.9 specimen contained three Ø8 transverse stirrups instead of two Ø10 stirrups, see Figure 6-c. All specimens were reinforced with four Ø10 longitudinal bars. However, the last test, referred to as the 9th POT, used two Ø12 and six Ø12 longitudinal bars instead of four Ø10.

Two of the three POT sample specimens, specifically POT-Ø10-16.8 and POT-Ø8-19.4, were designed for comparison with the third specimen, OS-17.9. Therefore, the POT samples were cast with nearly the same concrete compressive strength, differing by about 3 MPa. All samples maintained the same steel layout as OS-17.9, featuring three Ø8 and two Ø10 transverse stirrups along with four Ø10 longitudinal rebars.

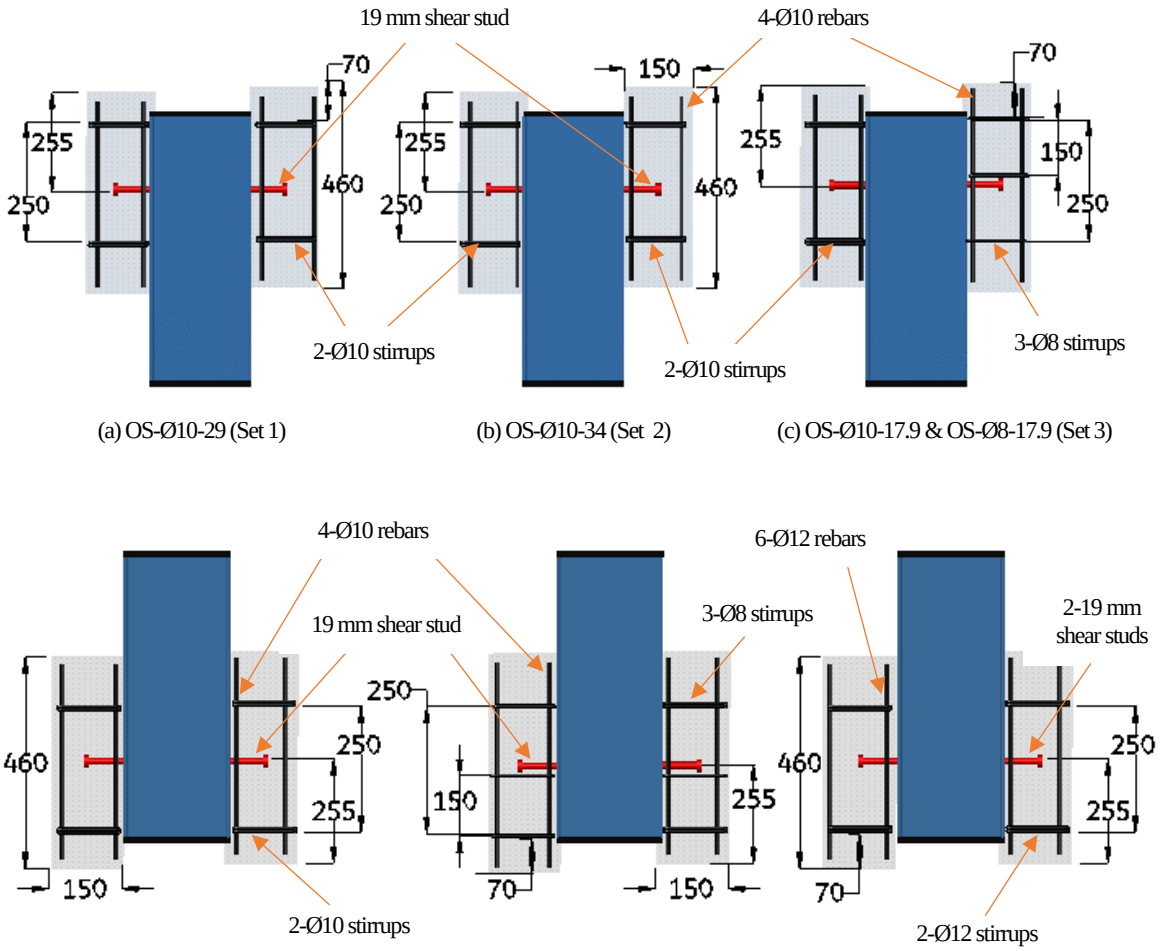

Figure 6. OSPOT and POT tests

3.2. Test Program

A total of nine tests were fabricated identically with the same geometrical configurations, as shown in Table 1.

Table 1. Parameters of push-out test specimens

No.		Specimen	f_c (MPa)	Test set-up	No. of studs (each side)	Testing age (Days)	Transverse reinforcement detail
1	Set 1	OS-Ø10-29-A	29	OSPOT	1	28	2-Ø10
2		OS-Ø10-29-B	29	OSPOT	1	28	2-Ø10
3	Set 2	OS-Ø10-34-A	34	OSPOT	1	28	2-Ø10
4		OS-Ø10-34-B	34	OSPOT	1	28	2-Ø10
5	Set 3	OS-Ø10-17.9	17.9	OSPOT	1	28	2-Ø10
6		OS-Ø8-17.9	17.9	OSPOT	1	28	3-Ø8
7		POT-Ø10-16.8	16.8	POT	1	28	2-Ø10
8		POT-Ø8-19.4	19.4	POT	1	28	3-Ø8
9		POT-Ø12-48	48	POT	2	21	2-Ø12

All the reinforced OS, POT-Ø8 and POT-Ø10 specimens had 4-Ø10 longitudinal rebars while POT-Ø12-48 reinforced by 6-Ø12.

The main variables of the tested specimens were the test setup, the consistency of results obtained from the POT and OSPOT, concrete compressive strength and the transverse rebars distribution. The specimens were initially divided according to the test setup, followed by the reinforcement and concrete compressive strength. Hence, the OSPOT samples were designated as OS- Ø-C (Ø is the diameter of the transverse stirrups and C is the cubic compressive strength of the concrete used in the test). For example, OS-Ø10-29 means one-slab POT, the transverse stirrups diameter is 10mm, and the cubic concrete compressive strength is 29 N/mm^2. The typical POTs were designated as POT-Ø-C at the same concepts. The tests were usually conducted on the 28th day after casting.

3.3. Material Properties

All the rebars in the testing campaign were grade B500B, conforming to BS 4449:2005. The shear stud tensile yield stress is 443 MPa and the ultimate strength is 523 MPa according to JIS G 3507-2010. For each batch of concrete mix, three 100 mm concrete cubes were cast simultaneously with the relevant specimens. The latter and the cubes were air-cured under the same environmental conditions to ensure consistency. The cubes were tested according to BS EN 12390-3:2009 on the same day as the relevant connectors.

3.4. Test Setup and Instrumentation

In the OSPOT configuration, a 25 mm thick steel plate was placed directly on the upper side of the concrete slab under evaluation to ensure uniform load distribution. Conversely, the specimens in the POT configuration were positioned on a 30 mm thick base plate to comply with BS-5 recommendations. A hydraulic jack with a capacity of 600 kN was employed to apply the load in both setups.

The testing procedure involved two distinct load steps for all tests conducted in both OSPOT and POT configurations: i) initially, the specimens were subjected to five loading and unloading cycles, reaching 40% of the anticipated failure load, with a load increment rate of 1 kN/s; ii) subsequently, a monotonic load was applied in displacement control, with an increment rate of 0.03 mm/s, until failure occurred.

A load cell was utilized to measure the applied load, while the relative movement between the steel section and the concrete slab in the load direction (slip) was monitored using an internal linear variable differential transformer (LVDT). In the OSPOT configuration, two additional LVDTs, positioned on either side at the midpoint of the slab, see Figure 7-a, A third LVDT was positioned at the back, attached to the untested slab, to monitor the stability of the specimen during the loading process, see Figure 7-b. The POT configuration utilized one LVDT at the center of each slab to monitor steel-concrete separation.

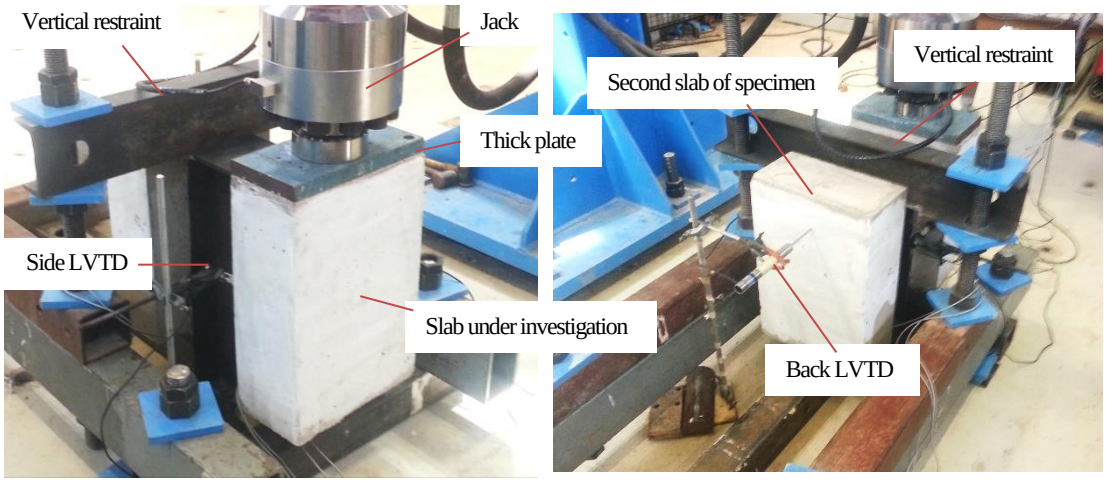

Figure 7. Tests setup and used instruments in OSPOT, (a) front view (d) back view

Data acquisition systems were employed to simultaneously record the applied load vs slip. Three specimens were evaluated using the standard POT method, which adheres to BS-5 specifications, while the remaining specimens were tested according to the improved OSPOT setup as explained in Para 2.3 above. In the OSPOT specimens, two steel end plates, each with a thickness of 12 mm, were welded to both the top and bottom of the steel section to ensure homogeneous load distribution resulting from the applied load and the consequent reaction at the base.

3.5. Concrete Production

For the push-out testing, BS-5 does not prescribe a specific casting method for the POT specimens; hence, a vertical casting in an inverted position to the load direction, to ensure that voids would not form under the studs on their bearing side [31]. This method of casting was adopted for all specimens in this study. The casting was in three layers and a vibration poker was used during the casting.

It is worth mentioning that Oehlers & Johnson (1987) [32] derived a formula that estimates the studs shear resistance, see Para 6, using the data of more than 100 POT tests. Most of the data were from Ollgaard et al. (1971) [31], who cast their samples vertically.

All the research specimens, i.e. both POT and OSPOT specimens, were designed with identical geometric specifications in which the concrete slab dimensions were 460 mm × 300 mm × 150 mm (height × width × thickness).

Concrete production in this study was conducted under laboratory conditions, allowing for greater control over the consistency of concrete properties across all castings. A fine natural aggregate (sand) with a granule size of 0-4 mm and a coarse aggregate (gravel) with a maximum size of 10 mm were selected for the concrete production. To assess the effect of concrete compressive strength on the shear resistance capacity of the shear studs connection, three types of ordinary concrete were utilized to show the relationship between varying concrete strengths and the shear resistance of the studs. Table 2 shows in detail the concrete mix proportions for each type of concrete grade.

Table 2. Proportion of different contents in the concrete mix design of shear studs tests

Concrete grade	Age of testing (days)	Cement	Fine aggregate	Coarse aggregate	Water	
C20	28	305	825	1008.8	270	kg/m^3
C30	28	368.5	907.5	1108.8	240	kg/m^3
C35	28	450	880	1100	260	kg/m^3

4. Results and Observations

Table 3 summarizes the overall results and describes the failure modes for the OSPOT and POT specimens, while Figure 8 shows the load-slip curves for all the tests. In all the OSPOTs, the applied load represents the shear connector resistance. In POTs, the stud shear resistance is equal to the applied load divided by the number of studs. Thus, the maximum load (Pu) is equal to the ultimate failure load for all the specimens.

Table 3. Tests, failure loads, slips and failure modes

	Test	P_u (kN)	P_u/ST (kN)	δ_u (mm)	δ_{uk} (mm)	Failure mode	
						Studs	Slabs
Set 1	OS-Ø10-29-A	90	90	7	14	Heavily deformed with a partial shearing off above the welded collar the	Excessive bearing failure around the studs plus four diagonal cracks from the back. No cracks at the fort of the slab. But the cracks at OS-Ø8-17.9 are less apparent. No visible cracks at the front.
	OS-Ø10-29-B	84	84	6	18		
Set 2	OS-Ø10-34-A	95	95	8	13		
	OS-Ø10-34-B	115*	115*	9	17		
		104	104				
Set 3	OS-Ø10-17.9	70	70	8	12	Stud at OS-Ø8-17.9 sheared off and deformed more than the other side in which no fracture was noticed	
	OS-Ø8-17.9	75	75	6	8		
POT- Ø10-16.8		210	105	11	19	Moderate Deformed. No shear off	Less bearing failure and the cracks at the back are less sever associated with cracks at the front.
POT- Ø8-19.4		220	110	14	22		
POT- Ø12-48		550	112.5	Specimen did not fail due to the limited capacity of the hydraulic jack			

δu represents the maximum elastic slip and δuk is the maximum slip.

* Result affected by the flange incasement.

4.1. Failure Modes and Cracks' Pattern

In the OSPOT specimens, no visible cracks were observed on the front side. Initially, cracks emerged at the rear, particularly in the vicinity of the shear stud, and propagated diagonally towards the edges of the slab. However, their progression was effectively restrained by the transverse stirrups. In the first set of observations, cracks became distinctly noticeable at an approximate slip of 10 mm. Additionally, concrete crushing was observed near the weld collar and around the shear stud, leading to significant separation of the slab. On the rear side of the slab, localized concrete crushing in front of the shear stud was evident. Typically, four radial cracks were clearly visible in the region surrounding the stud.

Following failure, the headed stud remained embedded within the concrete of the slabs, despite a complete separation between the slab and the beam, owing to the anchorage effect of the stud's head. However, a noticeable separation was clear between the steel section and the slab. In both sets of specimens, the slabs exhibited a similar failure mechanism, resulting in partial shear-out of the headed studs.

The crack pattern in the Ø8 studs was less pronounced than in the Ø10 studs, which may reflect the effect of using three transverse stirrups instead of two. The local crushing of the concrete that occurred in the OS-17.9 tests was associated with four visible radial cracks on the back side of the failed slab. At failure, the slab concrete of POT-Ø10 specimen separated from the steel section, but a higher level of separation was noted in the OSPOT samples. However, they remained bonded by the studs, which did not shear off. Cracks were clearly visible on the back of the specimen,

with crack lines extending toward the edges, similar to the OSPOT results, though less severe—no large pieces of concrete separated from the slab as observed in the OSPOT tests. An additional crack appeared on the front of the specimen in the lower third of the concrete slab, with signs of crushed concrete noticeable at the base of the specimen. All rebars in every specimen remained intact, showing no clear signs of deformation.

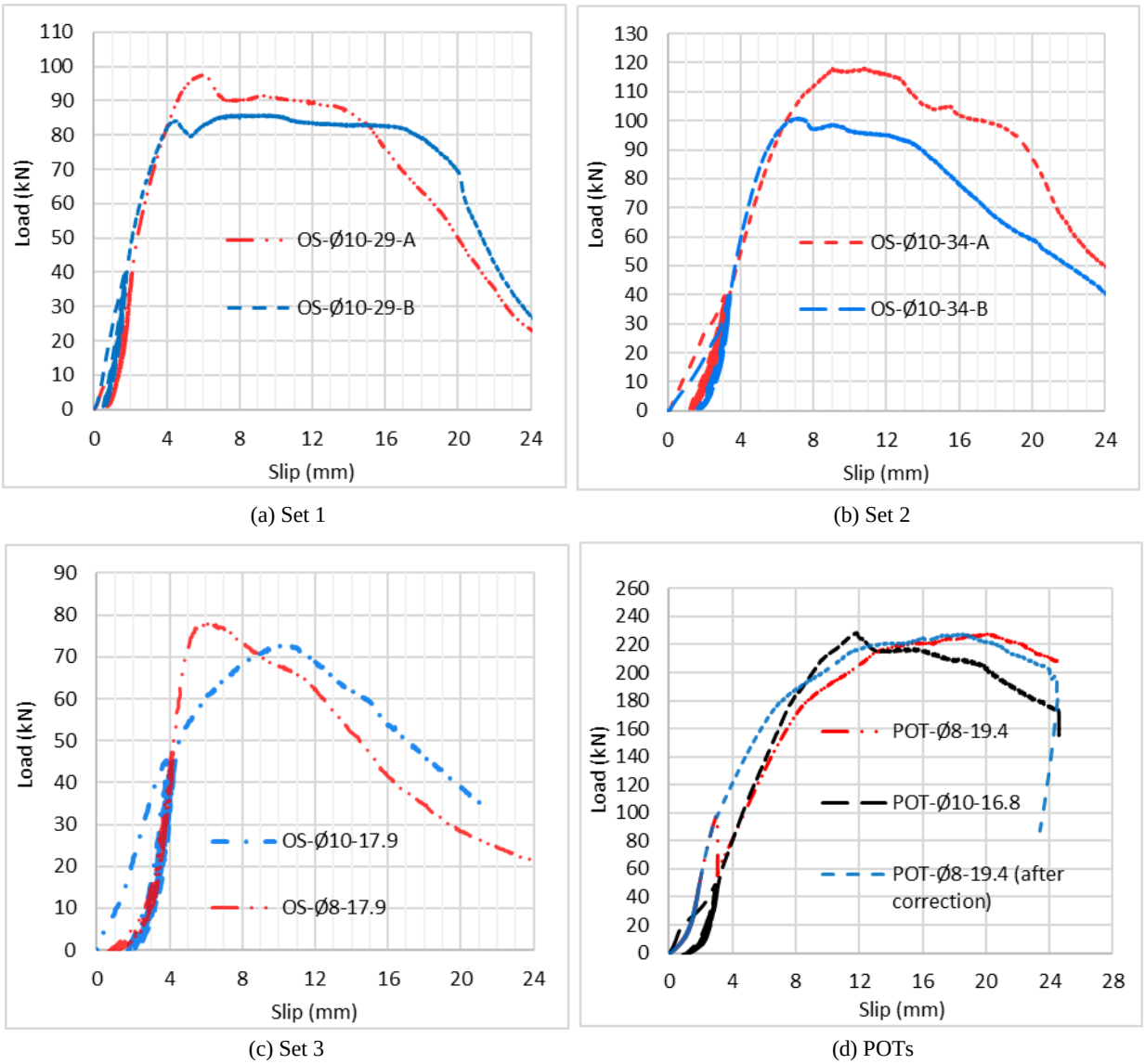

(a) Set 1

(b) Set 2

(c) Set 3

(d) POTs

Figure 8. Load-slip curves of all the test

4.2. Shear Studs Plastic Deformation

The fracture of the studs' shank occurred right above the welding in the first two sets. Examination of Set 3 revealed that the stud with a diameter of Ø8 was sheared right above the weld collar, whereas the Ø10 stud exhibited significant bending. A comparative analysis of the condition of the studs following the OSPOT and POT investigations indicated that those assessed during the latter exhibited less deformation. Notably, there was no incidence of shearing off for any stud; instead, the deformation was limited to bending in the load direction, despite the higher loads applied during the testing. This observation may support the observation which suggests that the studs in the POT configuration are subjected to a compressive force rather than a tensile force. The compressive force typically enhances the resistance of head studs [3], whereas tensile forces tend to reduce studs' resistance [17]. This might further support the conclusion that the studs in the newly modified OSPOT configuration demonstrate a pure shear behavior, without influence from normal forces. Additionally, the increased ductility observed in the OSPOT configuration aligns with Loh et al. (2004) [33] assertion that studs exhibit greater ductility under such conditions. For the POT-Ø12 configuration, the studs did not undergo any plastic deformation.

4.3. Load-Slip Behavior

In the first set, an initial plastic slip of 1mm occurred due to the sliding of the concrete slab over the steel section as a result of the applied load, however, when the load was removed the head studs were unable to retrieve all the vertical

displacement happened, in the load direction, leading to a *residual slippage or plastic slip* for the connection. In the final stage of loading, i.e. after the repeated loading, and starting from the residual slip, the Load-slip curves show an almost linear progression until about 90% of the maximum load. Notably, within the elastic range of both sets, Set 1 and Set 2, the behavior of the studs was remarkably similar, particularly under repeated loading conditions, and the permanent (plastic) slip was identical for the respective sets. Nonetheless, in the second set of experiments, an error occurred during the concrete casting of one of the slabs, resulting in a partial encasement of the flange within the concrete. This encased section was subjected directly to the applied load, thereby enhancing resistance to the load as the vertical movement of the slab was impeded by the encasement. The evidence of this interruption was clearly observable following the separation of the slab from the steel section, as the concrete in the encased area exhibited signs of crushing due to the direct loading.

The shear connections in the first two sets exhibited ductile behavior, see Figure 8, maintaining their shear resistance until the shear stud initial failure. This extended period of ductility, which significantly exceeded the EC-4 requirement of 6 mm, occurred because the shear stud did not fail suddenly. Instead, it bent gradually in the direction of the applied load until the shank began to fracture, at this point, the load capacity decreased sharply.

The residual slip in the second set increased to approximately 2 mm, compared to 1 mm in the first set. In Set 3, no residual slip was observed due to the relatively weak concrete (less than 18 MPa). The stud was able to return the cracked slab to its original position after reloading. However, this ability diminished as the strength of the concrete increased, as revealed by the results of the previous four OSPOT tests. Though the POT-Ø10-16.8 and POT-Ø8-19.4 samples failed at loads higher than expected, both curves demonstrated consistent behavior. Aside from the residual slip during repeated loading, the difference in shear resistance was minimal

4.4. Load-Slip Curves Expressions

Several authors have presented various numerical expressions to predict the load-slip relationship of the headed studs from the analysis of the POT results. Table 4 shows four expressions presented by Buttry (1965) [34], Ollgaard et al. (1971) [31], An & Cederwall (1996) [35] and Xue at el. (2008) [36]. In the first two equations, S is in inches, while S in the last two equations is mm. Figure 9 shows the predicated load-slip curves for the six OSPOTs conducted in this paper. These equations were derived from the results of POT tests, which typically used a concrete compressive strength of around 30 MPa. The load-slip curves for OS-29 and OS-34 are more consistent with the predictions compared to OS-19.7 during the plastic region. Overall, these expressions have provided valid predictions for the OSPOT testing, as illustrated in Figure 9.

Table 4. Load-slip predictions offered by authors

Authors	Prediction formula	Notations
Buttry (1965) [34]	$p = (\frac{80S}{1+80S})P_u$	P_u is the maximum shear load of the stud
Ollgaard et al. (1971) [31]	$p = (1 - e^{-18S})P_u$	P represent the shear load of the stud
An & Cederwall (1996) [35]	$p = (\frac{2.24(S-0.058)}{1+1.98(S-0.058)})P_u$	S is the slip when the load is equal to P
Xue et al. (2008) [36]	$p = (\frac{S}{0.5+0.97S})P_u$	

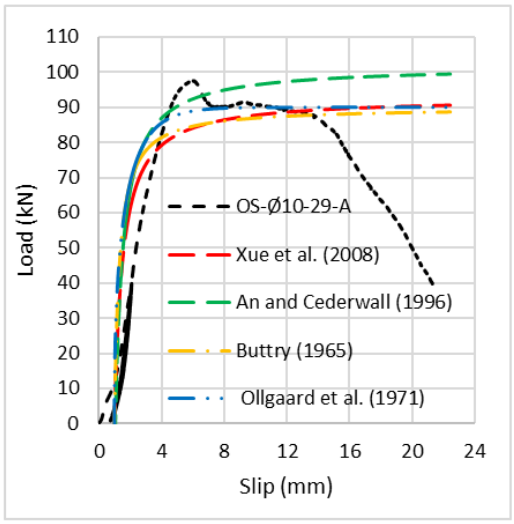

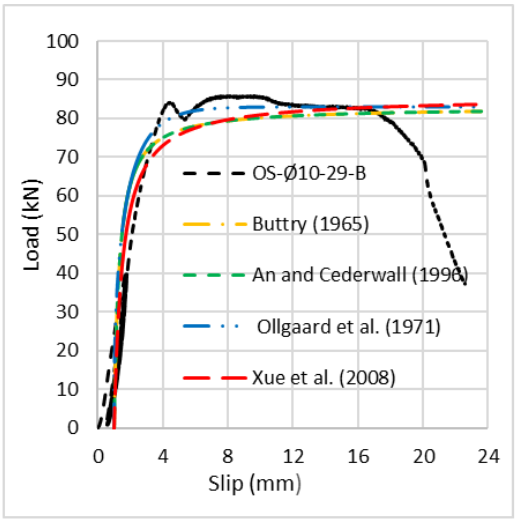

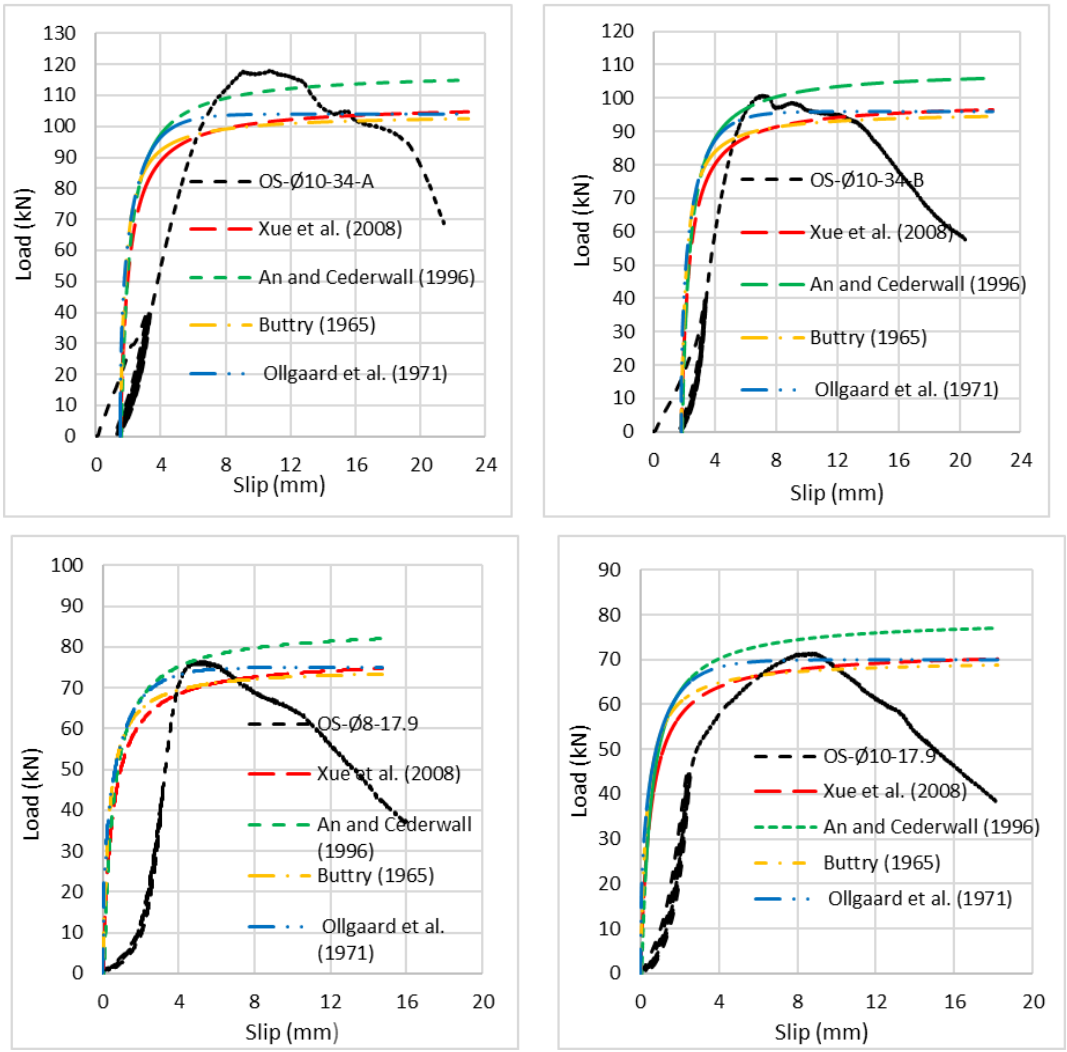

Figure 9. Load-slip curves of the OSPOTs vs empirical expressions

5. Discussion

The OSPOTs and POTs were conducted to facilitate the comparison between the POT and OSPOT and hence to validate the improved one-slab push-out test; explore the effect of the frictional reaction on the results; to investigate the effect of the compressive strength of the concrete and the redistribution of the transverse stirrups on the studs' shear resistance. Further, to compare the OSPOT experimental results with those published by other researchers.

5.1. OSPOTs vs. POTs Results

The results of the two OSPOTs- 29, i.e. Set 1, were consistent and the difference in shear resistance between the first set was about 4 kN and the average was about 87 kN per stud. The failure loads of identical twins, i.e. samples OSPOTs-34, were 98 and 115 kN due to the flange encasement of one side. Hence the difference was about 18 kN, and the mean is 107 kN, thus the stud resistance of 115 kN is still within the requirements of EC-4 Clause B.2.5 that considered the scatter in POTs result. This clause recommends, for evaluating POTs' results, "the deviation of any individual test result from the mean value obtained from all tests does not exceed 10%" as 1.1×107 equals to 117.7 kN. The expected resistance of this side was 102 kN which makes the average for this set 100 kN.

The shear resistance of the studs at POTs testing was also consistent with each other, i.e. 105 kN per stud for Ø10 and 110 kN for Ø8, however, they were higher than the studs' resistance in OS-Ø10-17.9 and OS-Ø8-17.9, i.e. 70 kN and 75 kN respectively.

The results of these two tests may confirm the observation reported by Oehlers & Johnson (1987) [32] about the effect of the frictional resistance under the slab that increases the stud's shear resistance. In fact, applying their suggested reduction factor of 19%, the shear resistance becomes 85kN and 89kN which are closer to both the OSPOT and the predictions offered by the BS-5, EC-4 and other predictions.

Furthermore, the formwork of POT-Ø8 specimen moved during the vibration of the concrete causing a partial encasement for one side of the steel beam into the concrete. Despite the sudden drop in loading due to the crushing of concrete under the encased flange, from 100 to about 40 kN, because of the crushing of the concrete. The drop in loading

was toward the POT-Ø10 curve. In Figure 8-c corrected curve maintains almost the same elastic stiffness also the curve from the test, i.e. without correction, maintains the same stiffness across most of the elastic limit of the two specimens. The POT-Ø8 test shows clearly that the POT results are the average of the shear resistance of the two sides even though one of them might be weaker, in other words, the POT results do not represent the individual shear resistance of the connector, which is contrary to the OSPOT procedure.

The expected failure load for POT-Ø12 was about 500 kN. However, up to 515 kN, the POT sample depicted minor signs of cracks, and the sample did not fail. The actuator could not reach its designed maximum load, which was 600 kN, and the test had to be terminated at 515 kN.

5.2. Concrete Compressive Effect

The compressive strength of the concrete clearly influences the elastic range of the specimen. By comparing the three tests reinforced with Ø10 stirrups—specifically the identical specimens OS-Ø10-29, OS-Ø10-34, and OS-Ø10-17.9—it is evident that higher concrete compressive strength significantly impacts the structural behavior of the shear stud. The elastic range nearly extends to the ultimate load, followed by a distinct ductility plateau and an increase in shear resistance, see Figure 8.

Further, Figure 8 shows that the stiffness of the first two specimens slightly increased compared to OS-Ø10-17.9 due to the higher concrete compressive strength, supporting the conclusions of Rambo-Roddenberry (2002) [12] and other researchers that the elastic stiffness of the headed stud connection is directly proportional to the concrete compressive strength. In fact, since the difference in concrete compressive strength between the first two sets was minimal—approximately 5 MPa—the resulting elastic stiffness is nearly identical.

5.3. Rebars Redistribution Effect

Previous studies have explored the impact of varying the area of reinforcement steel on shear resistance, such as the works by Johnson & Oehlers (1981) [32] and Xue et al. (2008) [36]. Specifically, Johnson & Oehlers (1981) [32] demonstrated that reinforced post-tensioned (POT) specimens exhibit greater shear resistance and ductility compared to non-reinforced specimens. To the best of the author's knowledge, few studies have investigated the effect of redistributing transverse rebars while keeping the overall area of the rebars constant, i.e. ρ_t is constant, on the shear resistance of headed studs, as illustrated by the OS-19.7 tests.

The steel area for two rebars with a diameter of 10 mm is approximately 157 mm², which is nearly the same as the steel area for three rebars with a diameter of 8 mm, totalling 150 mm². Therefore, the steel layout of 2-Ø10 can be substituted with 3-Ø8 transverse stirrups while maintaining a similar steel ratio (ρ_t). The 4-Ø10 longitudinal bars remain unchanged as shown in Figure 6-c.

The results for the OS-Ø10-17.9 and OS-Ø8-17.9 samples clearly demonstrate the impact of rebar redistribution on both shear resistance and ductility of the connection. The overall shear resistance in the two samples shows only a small difference of about 5 kN, which can be considered a normal variance between the two samples from the same set. However, the elastic range in the Ø8 sample is nearly double that of its Ø10 counterpart, see Figure 8-c. A lesser effect of transverse rebar distribution was observed in the POT specimens, specifically POT-Ø10-16.8 and POT-Ø8-19.4. This discrepancy may be attributed to the testing setup. Nevertheless, further investigation is needed to confirm the effects of rebar redistribution on the structural performance of shear studs in concrete with varying compressive strengths.

5.4. A Comparison Between the Increase of the Steel Ratio and the Rebars Re-Distribution

In Xue et al. (2008) [36] POTs, the shear resistance of the specimen, which employs 16mm-headed studs, is enhanced by the increase of the reinforcement ratio; however, the shear resistance of the specimen which employed 13mm-suds only showed a minor change. Adding twice the area of reinforcement, in this case, an extra two layers of Ø10 rebars, enhanced the shear resistance by 13% for studs of 16 mm in diameter, and only 5 % for 13mm studs.

In this study, the redistribution of the transverse rebars increases the shear resistance by about a 7%. Furthermore, no obvious effect was found for doubling the area of reinforcement on the elasticity range of 16mm studs in the work conducted by Xue et al. (2008) [36] compared to the clear effect of using thinner rebars to improve the sample elastic behavior that is demonstrated in this study.

6. Estimations of Headed Studs' Shear Resistance

Ollgaard et al. (1971) [31] suggested that the stud's shear resistance (f_{vs}) isthe lesser of the following two numerical expressions below. These expressions were derived from the POTs investigation of specimens with 16 mm and 19 mm shear studs.

$$f_{vs} = c_1\sqrt{f_c' E_c A_{sc}} \quad (1)$$

$$f_{vs} = c_2 f_{uc} A_{sc} \quad (2)$$

where: C_1 & C_2 are calibration factors from the tests; f_c' is the compressive strength of concrete; E_c is the concrete elastic modulus, A_{sc} is the cross-sectional area of the shank of the stud; and f_{uc} is the ultimate tensile strength of the shear connector.

Different code of practices and design specifications use different values for C_1 & C_2 to evaluate the nominal strength of shear connectors as shown in Table 5 [17].

Table 5. Factors C1 and C2 in different design specifications [17]

	AS 2327.1 (2003)	Eurocode 4 (2004)	DIN V18800-5 (2004)	DIN-Richtlinien (1981)	AISC- Manual (2001)	CSA S16-01 (2001)
C_1	0.39	0.37	0.32	0.32	0.50	0.40
C_2	0.80	0.80	0.80	0.70	1.00	0.80

Oehlers & Johnson (1987) [32] presented Equation 3. In comparison with the predictions of Ollgaard et al. (1971) [31], Equation 3 highlights the interaction between the concrete and steel properties in a better way and defines the effect of the stud's number on the POT results

$$f_{vs} = 4.1 \left[\frac{f_{cu}}{f_{uc}}\right]^{0.35} \left[\frac{E_c}{E_{sc}}\right]^{0.4} A_{sc}\ f_{uc} \quad (3)$$

In which f_{cu} is the cubic compressive strength of concrete; E_{sc} , E_c are the modulus of elasticity of stud's material and concrete respectively. It is worth mentioning that, Equation 3 shaped the outline for the stud strengths given in BSI [37] shown in Table 6 [17]. The shear resistance represents a linear regression line through POTs results.

Table 6. British Standard BSI [37] recommendation for headed studs shear resistance

Dimensions of stud shear connectors		Characteristic strength of concrete				
Nominal shank diameter	Nominal height	As-welded height	N/mm^2 25	N/mm^2 30	N/mm^2 35	N/mm^2 40
mm	mm	mm	kN	kN	kN	kN
25	100	95	146	154	161	168
22	100	95	119	126	132	139
19	100	95	95	100	104	109
19	75	70	82	87	91	96
16	75	70	70	74	78	82
13	65	60	44	47	49	52
NOTE 1 For concrete of characteristic strength greater than 40 N/mm^2 use the values for 40 N/mm^2.						
NOTE 2 For connectors of heights greater than tabulated use the values for the greatest height tabulated.						

The shear resistance, in Table 5, is a function of the stud's diameter and length, i.e. dimensions of the stud shear connectors, against the compressive cube strength of the concrete where the studs are embedded.

Xue et al. (2008) [36] and Shen & Chung (2016) [30] developed Equation 3 by analysing the stud's shear mechanism in push-out tests and suggested Equations 4 and 5 respectively.

$$f_{vs} = \left(5.3 - \frac{1.3}{\sqrt{n}}\right) \left[\frac{f_{cu}}{f_{uc}}\right]^{0.35} \left[\frac{E_c}{E_{sc}}\right]^{0.4} A_{sc}\ f_{uc} \quad (4)$$

$$f_{vs} = 3 \left[\frac{f_{cu}}{f_{uc}}\right]^{0.35} \left[\frac{E_c}{E_{sc}}\right]^{0.4} A_{sc}\ f_{uc} \quad (5)$$

wherein n is the number of the studs on one side of the specimen.

The estimates provided by authors and standards for shear resistance specify limits on the dimensions and strength of studs, as well as the welding layout and the required strength of the concrete medium. These limitations ensure that the intended failure mode is shearing of the studs, allowing them to behave sufficiently in a ductile manner. This approach helps prevent premature failure modes, such as concrete splitting or stud pull-out.

7. Data Base

Numerous push-out tests have been conducted by various researchers, including Hicks & McConnel (1997) [9], Galjaard & Walraven (2001) [38], Lam & El-Lobody (2005) [39], Shen (2013) [40], Shen & Chung (2017) [30] and Kumar & Chaudhary (2019) [41], to investigate shear studs with different diameters. Table 7 specifically presents the results of tests conducted on 19 mm head studs, 114 tests are included in this table, which encompasses eight tests carried out in this research. Table 6 lists, also, the reference names of the specimens along with the size of the shear studs. All these tests are compared against the predictions from BS-5, EC-4, Oehlers & Johnson (1987) [32], and Xue et al. (2008) [36], i.e. Equations 3 and 4. In Figures 10 and 11, the test results are plotted against the four predictions to highlight the accuracy of these estimates.

Table 7. Push-out tests' configurations conducted by researchers

No.	Author (s)	Specimens	Specimen Size (Height×width×thickness)	Testing method	Shear studs arrangement (side)	Stud's height (mm)	Es (MPa)	F_{uc} (MPa)	Ec (MPa)	F_{cu} (MPa)	Test results (kN)	Bs-5 (kN)	Ec-4 (kN)	Oehlers et al. (1987) (kN)	Xue et al. (2008) (kN)
1	An & Cederwall (1996) [35]	NSC11	625×600×150	POT	4 studs	75	207	519	31	38	115	94	101	110	122
2		NSC12							31	39	112	94	102	111	123
3		NSC21							31	39	121	94	102	111	123
4		NSC22							32	40	119	96	106	114	125
5	Lyons et al. (1994) [42]	14	914×914×146	POT	2 studs	101.6	200	461	21	26	95	97	70	78	90
6		15							21	26	101	97	70	78	90
7		37							30	52	115	109	105	114	119
8		38							30	52	108	109	105	114	119
9		39							30	52	108	109	105	114	119
10		40							30	52	105	109	105	114	119
11		41							30	52	107	109	105	114	119
12		42							30	52	109	109	105	114	119
13	Hicks et al. (1997) [9]	4S-ORB1	900×750×120	Vertical OSPOT (with slide)	4 studs	100	NA	NA	15	37	79	**106**	**69**	78	85
14		4S-ORB2							14	31	90	**101**	**64**	71	80
15		4S-FB1		POT	5 studs				15	37	107	**106**	**69**	78	85
16		4S-FB2							14	31	118	**101**	**64**	71	80
17	Lam (2007) [43]	RC1	1200×1600×150	Horizontal OSPOT	6 studs	100	200	450	16	15	72	**95**	60	79	72
18		RC2							23	29	103	**100**	89	113	93
19		RC3							22	29	102	**100**	88	112	92
20		RC4							22	28	100	**100**	87	111	91
21		RC5							30	50	133	**109**	114	152	115
22	Xue et al. (2008) [36]	STUD 13	494×254×120	POT	1 stud	103	200	444.4	33	51	111	109	101	115	119
23		STUD 14								51	111	109	101	115	119
24		STUD 15								51	110	109	101	115	119
25		STUD 16							29	38	101	107	98	99	107
26		STUD 17								38	101	107	98	99	107
27		STUD 18								38	104	107	98	99	107
28	Galjaard et al (2001) [38]	C30/37	650×600×200	POT	4 studs	125	NA	NA	27	41	120	109	99	100	108
29										41	113	109	99	100	108
30										41	113	109	99	100	108
31		C70/85							42	99	127	109	104	163	154
32										99	129	109	104	163	154
33		LC30/37							29	47	102	109	104	108	114
34										47	111	109	104	108	114
35		LC62/78							38	83	125	109	104	147	143
36										83	128	109	104	147	143
37	Topkaya et al. (2004) [21]	28 days	915×610×203	Horizontal OSPOT	2 studs	127	200	460	28	35	93	104	94	97	107
38									28	35	93	104	94	97	107
39									28	35	93	104	94	97	107
40		14 days							28	35	94	104	94	97	107
41									28	35	89	104	94	97	107
42									28	35	85	104	94	97	107
43		7 days							27	33	88	98	89	93	104
44									27	33	90	98	89	93	104
45									27	33	82	98	89	93	104
46	Lam & El-Lobody (2005) [39]	SP1	619×469×150	POT	1 stud	100	200	470.8	17	50	130	109	86	91	95
47		SP2							11	20	72	95	43	55	66
48		SP3							13	30	93	100	59	69	78
49		SP4							14	35	97	104	66	75	83
50	Lam & El-Lobody (2005) [39]	C25	PARAMETRIC STUDY	POT	1 stud	101	200	470.8	12	25	80	95	51	62	72
51		C30							13	30	90	100	59	69	78
52		C35							14	35	99	104	66	75	83
53		C40							15	40	106	109	73	80	87

54	Valente (2007) [7]	KBPD19.1	300×350×150	Vertical OSPOT-	1 stud	100	200	534	27	63	156	109	121	128	132
55		KBPD19.2						534	27	63	161	109	121	128	132
56		CN 19.1	650×600×150	POT	4 studs	100		594	25	63	141	109	117	133	140
57		CN 19.2						594	25	66	140	109	119	135	140
58		CN 19.3						594	25	65	139	109	119	135	141
62	Loh et al. (2004) [33]	1	650×600×150	POT (one slide)	4 studs	100	200	523	22	22	118	95	80	80	96
63		2							22	22	108	95	80	80	96
64		3							22	22	94	95	80	80	96
65	Rambo-Rodd (2002) [12]	1	914×614×146	POT (10% normal force)	2 studs	101.6	200	447.81	28	30	115	98	85	89	100
66		2							28	30	128	98	85	89	100
67		3							28	30	114	98	85	89	100
68		4							28	30	126	98	85	89	100
69		5							28	30	112	98	85	89	100
70		6							28	30	115	98	85	89	100
71		7							28	30	102	98	85	89	100
72		8							28	30	119	98	85	89	100
73		9							28	30	122	98	85	89	100
74		10							28	30	116	98	85	89	100
75		11							28	30	113	98	85	89	100
76		12							27	30	109	98	84	88	99
77	Shen (2013) [40]	SS 01	650×600×150	POT	4 studs	100	200	500	30	37	130	**85**	98	106	118
78		SS 02							29	35	140	**85**	94	103	115
79		SS 03							28	35	146	**85**	92	101	113
80		SS 04							27	36	138	**85**	92	101	112
81	Shen & Chung (2017) [30]	SS-01	650×600×125	POT	4 studs	100	205	507.8	24	35	126	104	115	96	107
82		SS-02							24	35	124	104	115	96	107
83		SS-03							24	35	123	104	115	96	107
84		SS-04							24	35	142	104	115	96	107
85		SS-05							24	35	136	104	115	96	107
86		SS-06							24	35	133	104	115	96	107
87	Kumar & Chaudhary (2019) [41]	C1-0RL0S0	460×300×150	POT	1 stud	100	NA	NA	25	33	117	102	84	97	110
88		C2-0RL0S0							27	39	126	106	95	106	118
89		C1-1RL0S25							25	33	137	102	84	97	110
90		C1-1RL0S50							25	33	131	102	84	97	110
91		C1-1RL0S75							25	33	124	102	84	97	110
92		C1-1RL1S100							25	33	119	102	84	97	110
93		C2-1RL0S25							27	39	138	106	95	106	118
94		C2-1RL0S50							27	39	132	106	95	106	118
95		C2-1RL0S75							27	39	127	106	95	106	118
96		C2-1RL0S100							27	39	122	106	95	106	118
97		C1-2RL100S25							25	33	138	102	84	97	110
98		C1-2RL80S25							25	33	141	102	84	97	110
99		C1-2RL60S25							25	33	146	102	84	97	110
100		C1-2RL100S50							25	33	136	102	84	97	110
101		C2-2RL100S25							27	39	146	106	95	106	118
102		C2-2RL80S25							27	39	152	106	95	106	118
103		C2-2RL60S25							27	39	159	106	95	106	118
104		C2-2RL100S50							27	39	144	106	95	106	118
105		C1-3RL50S25							25	33	153	102	84	97	110
106		C2-3RL50S25							27	39	162	106	95	106	118
107	This paper	OS-Ø10-29-A	460×300×150	OSPOT	1 stud	80	200	523	25	29	90	95	93	96	109
108		OS-Ø10-29-B							25	29	84	88	87	89	109
109		OS-Ø10-34-A							27	34	95	90	92	92	116
110		OS-Ø10-34-B							27	34	104	99	101	101	116
111		OS-Ø10-17.9							20	18	70	77	62	70	90
112		OS-Ø8-17.9							20	18	75	82	66	75	90
113		POT- Ø10-16.8	460×300×150	POT	1 stud				19	17	105	82	53	70	88
114		POT- Ø8-19.4							21	19	110	82	59	76	93

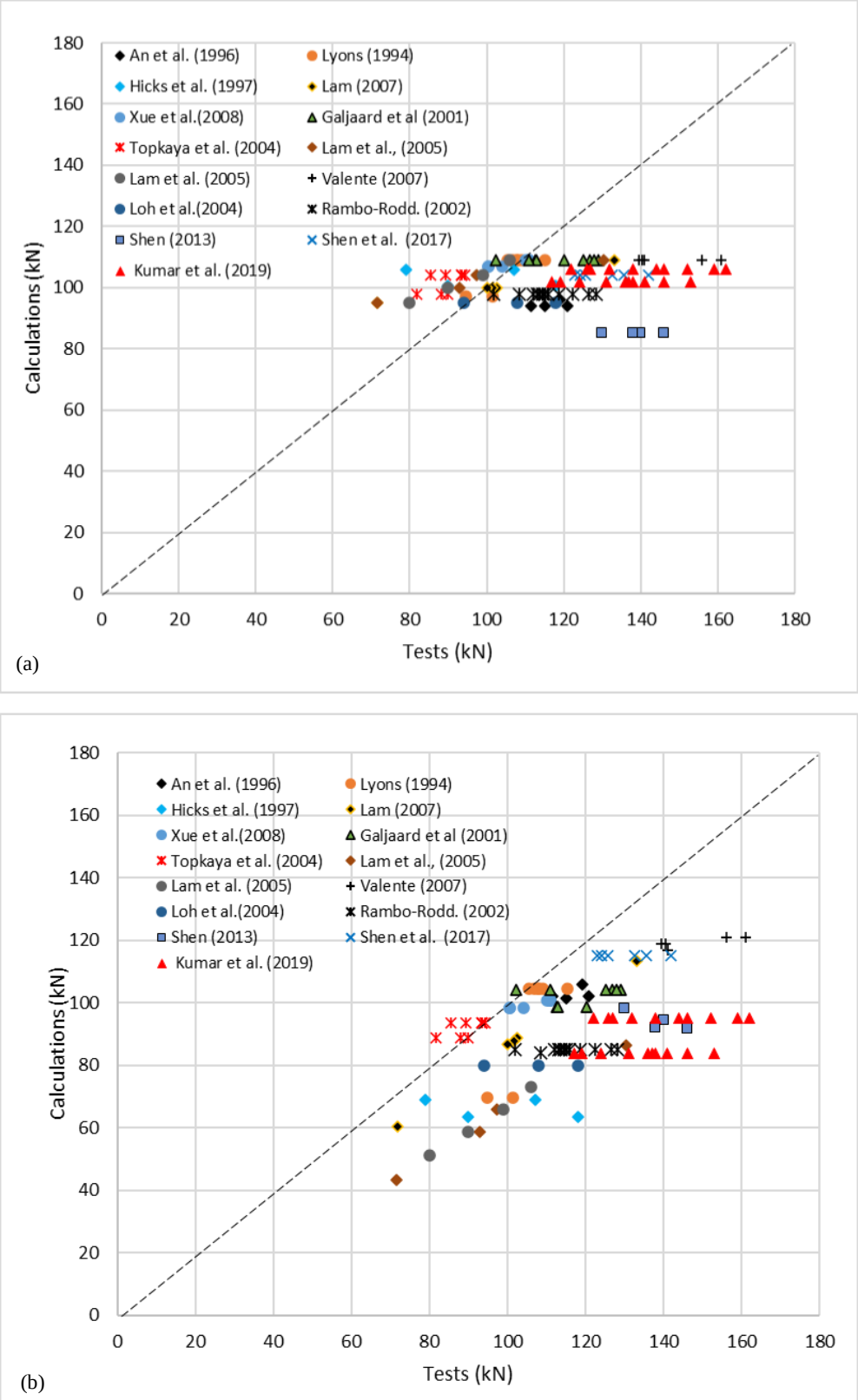

Figure 10. Researchers' vs (a) BS-5 and (b) EC-4 predications

Figure 11 illustrates the test results plotted against the four predictions to highlight the consistency with these estimates. Figure 11 shows that the one-slab horizontal push-out tests, such as those of Topkaya et al (2004) [21]. and Lam et al (2007) [43]. are generally more consistent with certain predictions, i.e. the EU-4, as well as Oehlers & Johnson (1987) [32] However, they do not align as well with the other two predictions. In horizontal (OSPOT), the frictional reaction is eliminated, resulting in more consistent outcomes. The POT results listed in Table 6 are, in general, scattered around the four predictions.

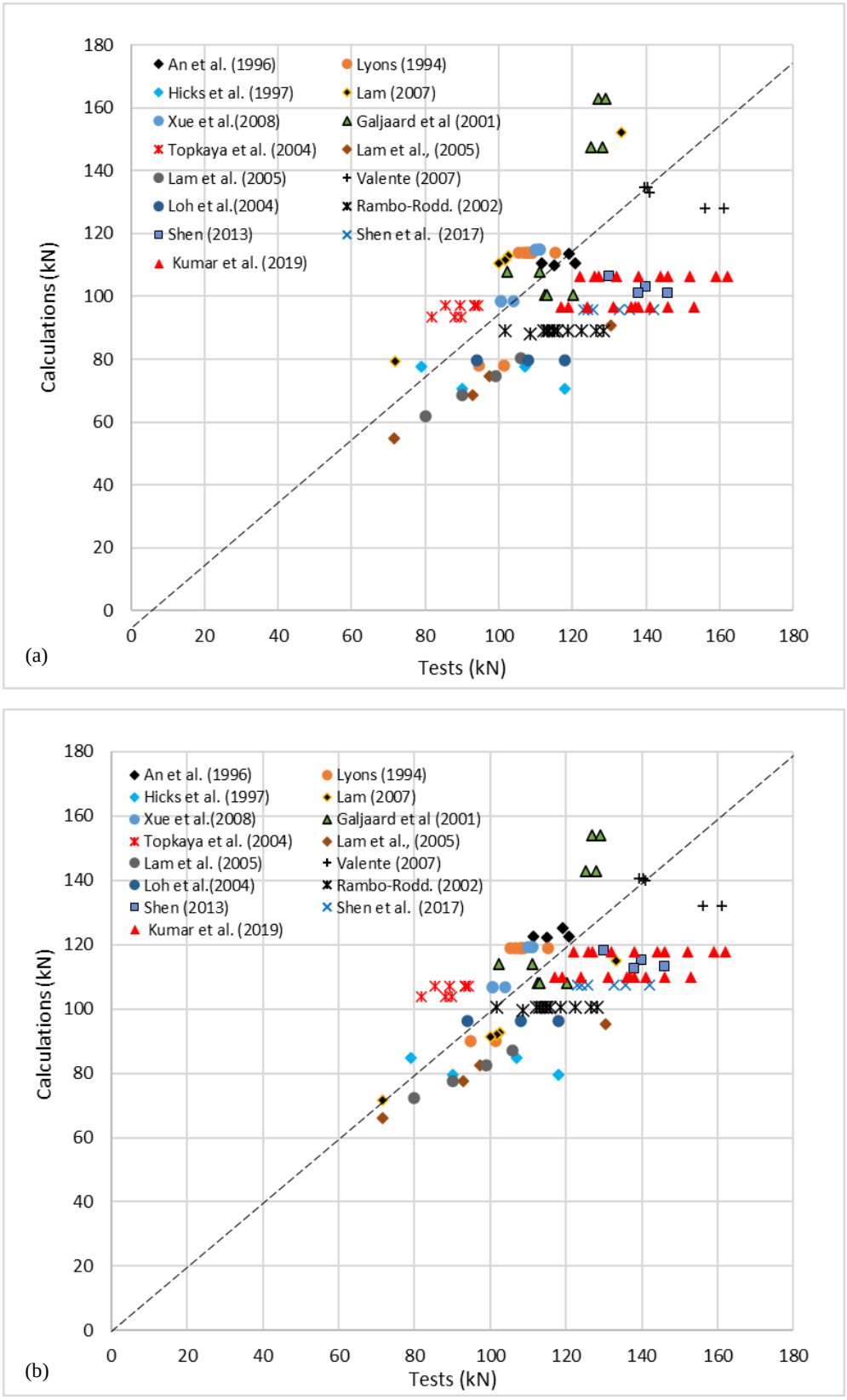

Figure 11. Researchers' vs (a) Equation 3 and (b) Equation 4

In Figure 12, the OSPOT results, contrary to POTs carried out in this research, are more consistent with BS-5, EU-4 and Oehlers & Johnson (1987) [32] predictions rather than Xue et al (2008) [36]. The POT predictions are typically obtained from the regression analysis of POTs' results. The number of tests affects the accuracy of the regression analysis. Xue et al (2008) [36] investigated only 30 POTs compared with 100 tests Oehlers & Johnson (1987) [32] used. The analysis of the results presented in Table 6, Figures 11 and 12 suggests that the newly improved OSPOT in this study might represent more accurately the characteristic behavior of the shear studs than the different setups.

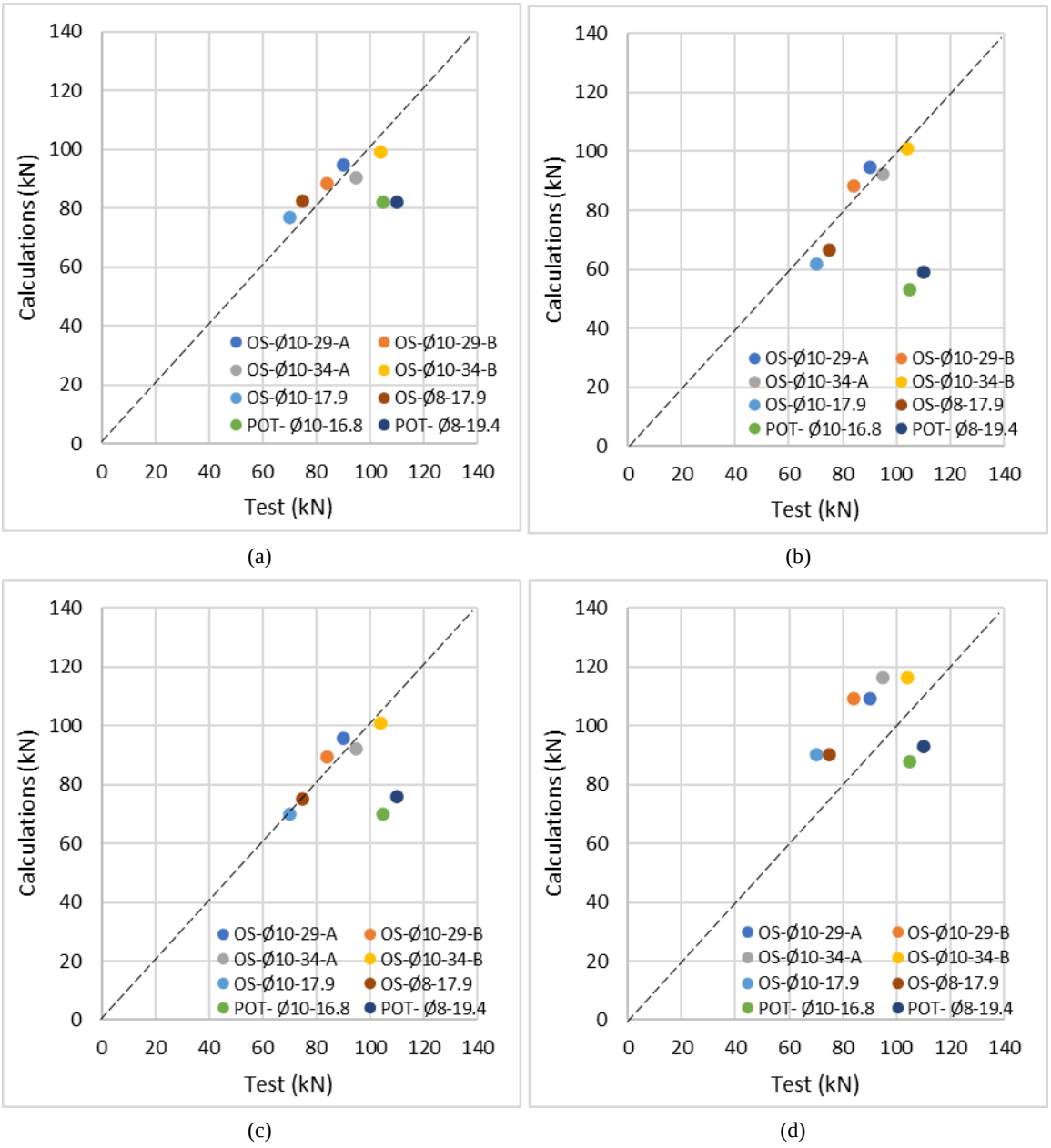

Figure 12. This research tests vs (a) BS-5, (b) EC-4, (c) Equation 3 and (d) Equation 4 predictions

8. Conclusions

In this study, six one-slab push-out tests (OSPOT) in a developed setup and three conventional push-out tests (POT) were conducted, and the results obtained from these tests were compared against each other. The work conducted in many studies was then evaluated against the studs' shear resistance estimation offered by BS-5, EC-4, and the equation for shear resistance presented by Oehlers & Johnson (1987) [32] and Xue et al (2008) [36]. From these investigations, the following conclusions can be drawn:

- The POT results in this study, which are performed on a solid base according to the BS-5 recommendations, without horizontal restraint, are about 20% higher than the OSPOT due to the test setup.
- This research's OSPOT results are in good agreement with horizontal OSPOT results, and OSPOT results are in better agreement with BS-5, EC-4, and Oehlers & Johnson (1987) [32] predictions than the POTs results compared to the horizontal setup.
- The Load-slip curves obtained from the proposed OSPOT noticeably show a higher degree of ductility, which may simulate the real load-slip relationship in full-scale composite beams, where the shear studs demonstrate a ductile behavior.
- The concrete compressive strength (f_c) affects the shear resistance obtained OSPOT similar to the f_c effects on POT results.

- The distribution of the area of the transverse steel from Ø10 to Ø8, for the same steel ration (ρ_t), i.e., transverse stirrups, increases the shear resistance of the headed stud, about 7%, and affects the elastic behavior of the specimen significantly, about 45%, which might be beneficial to consider in the design of the steel layout of the beam. However, more investigations are needed to confirm this observation for the shear studs which are embedded in concrete of compressive strength of 30MPa and more.
- POT results are the average of the shear resistance of the two concrete sides of the specimen even though one of them might be weaker. In other words, the POT results do not represent the individual shear resistance of the connector, which is contrary to the OSPOT procedure.
- The proposed new method of testing, i.e., OSPOT, has a significant potential to reduce the time and cost of the testing campaign, also increasing the number of tests as two results can be obtained from one POT specimen.

9. Declarations

9.1. Author Contributions

Conceptualization, M.A. and L.Sh.; methodology, L.SH. and M.A.; experimental campaign, M.A.; validation, L.Sh. and M.A.; formal analysis, M.A. and L.Sh.; investigation, L.Sh. and M.A.; resources, L.Sh. and M.A; data curation, L.Sh. and M.A; writing—original draft preparation, M.A. and L.Sh.; writing—review and editing, L.Sh. and M.A.; visualization, M.A. and L.Sh.; supervision, L.Sh. and M.A.; project administration, M.A.; funding acquisition, L.Sh. All authors have read and agreed to the published version of the manuscript.

9.2. Statement of Originality

This is the extended paper of "A Novel One-Sided Push-Out Test for Shear Connectors in Composite Beams" by Al-Shuwaili, M.; Palmeri, A.; Lombardo, M. which was presented in the 12th International Conference on Advances in Steel-Concrete Composite Structures. ASCCS 2018.

9.3. Data Availability Statement

The data presented in this study are available in the article.

9.4. Funding and Acknowledgments

The experimental campaign of this research was conducted at the School of Architecture, Building and Civil Engineering at Loughborough University-UK. The financial support was provided by Kufa University-Iraq for the experimental campaign. Both universities are gratefully acknowledged.

9.5. Conflicts of Interest

The authors declare no conflict of interest.

10. References

[1] Hadi, B. A., & Saleh, S. M. (2023). Behavior of Steel–Lightweight Self-Compacting Concrete Composite Beams with Various Degrees of Shear Interaction. Civil Engineering Journal (Iran), 9(11), 2689–2705. doi:10.28991/CEJ-2023-09-11-04.

[2] Jun, C., Shaoqian, W., Xuebing, Z., Hui, X., Fu, X., Yuqing, L., Caiqian, Y., Qing, X., Huaping, W., Faxing, D., & Ping, X. (2023). Investigations on the shearing performance of composite beams with group studs. Advances in Structural Engineering, 26(10), 1783–1802. doi:10.1177/13694332221120083.

[3] Nethercot, D. A. (1996). Composite steel and concrete structural members: fundamental behaviour. Engineering Structures, 18(11), 886. doi:10.1016/0141-0296(96)84811-5.

[4] Gyawali, M., Sennah, K., Ahmed, M., & Hamoda, A. (2024). Experimental study of static and fatigue push-out test on headed stud shear connectors in UHPC composite steel beams. Structures, 70. doi:10.1016/j.istruc.2024.107923.

[5] Yu, J., Wang, Y.-H., Li, C.-Y., Tan, J.-K., Yu, Z., & Shen, Q.-W. (2025). Experimental study of PZ shear connectors in composite beams. Structures, 75, 108616. doi:10.1016/j.istruc.2025.108616.

[6] Shahabi, S. E. M., Sulong, N. H., Shariati, M., & Shah, S. N. R. (2016). Performance of shear connectors at elevated temperatures-A review. Steel and Composite Structures, 20(1), 185-203. doi:10.12989/scs.2016.20.1.185.

[7] Valente, I. (2007). Experimental studies on shear connection systems in steel and lightweight concrete composite bridges. PhD Thesis, University of Minho, Braga, Portugal.

[8] Al-Shuwaili, M. A. (2018). Analytical investigations to the specimen size effect on the shear resistance of the perfobond shear connector in the push-out test. Procedia Structural Integrity, 13, 1924–1931. doi:10.1016/j.prostr.2018.12.269.

[9] Hicks, S. J., & McConnel, R. E. (1997). The shear resistance of headed studs used with profiled steel sheeting. Composite construction in steel and concrete III, 9-14 June, 1996, Irsee, Germany.

[10] Hicks, S. J., & Smith, A. L. (2014). Stud shear connectors in composite beams that support slabs with profiled steel sheeting. Structural Engineering International: Journal of the International Association for Bridge and Structural Engineering (IABSE), 24(2), 246–253. doi:10.2749/101686614X13830790993122.

[11] Nellinger, S., Odenbreit, C., Obiala, R., & Lawson, M. (2017). Influence of transverse loading onto push-out tests with deep steel decking. Journal of Constructional Steel Research, 128, 335–353. doi:10.1016/j.jcsr.2016.08.021.

[12] Rambo-Roddenberry, M. D. (2002). Behavior and strength of welded stud shear connectors. Ph.D. Thesis, Virginia Polytechnic Institute and State University, Blacksburg,, United States.

[13] Lorenc, W., Kubica, E., & Kozuch, M. (2010). Testing procedures in evaluation of resistance of innovative shear connection with composite dowels. Archives of Civil and Mechanical Engineering, 10(3), 51–63. doi:10.1016/s1644-9665(12)60136-8.

[14] BS 5400-5:2005. (2005). Steel, concrete and composite bridges - Code of practice for design of composite bridges. British Standards Institution (BSI), London, United Kingdom.

[15] EN 1994-2. (2005). Eurocode 4: Design of composite steel and concrete structures – Part 2: General rules and rules for bridges. European Committee for Standardization, Brussels, Belgium.

[16] Döinghaus, P. (2002). On the interaction of high-strength building materials in composite beams. Ph.D. Thesis, RWTH Aachen University, Aachen, Germany. (In German).

[17] Ernst, S. (2006). Factors affecting the behaviour of the shear connection of steel-concrete composite beams. Ph.D. Thesis, University of Western Sydney, Sydney, Australia.

[18] Patrick, M. (2000). Experimental investigation and design of longitudinal shear reinforcement in composite edge beams. Progress in Structural Engineering and Materials, 2(2), 196-217. doi:10.1002/1528-2716(200004/06)2:2<196::AID-PSE22>3.0.CO;2-2.

[19] Lam, D. (2002). New Test for Shear Connectors in Composite Construction. Composite Construction in Steel and Concrete IV, 404–414. doi:10.1061/40616(281)35.

[20] Zaki, R., Clifton, G. C., & Butterworth, J. W. (2003). Shear stud capacity in profiled steel decks. New Zealand Heavy Engineering Research Association, Auckland, New Zealand.

[21] Topkaya, C., Yura, J. A., & Williamson, E. B. (2004). Composite Shear Stud Strength at Early Concrete Ages. Journal of Structural Engineering, 130(6), 952–960. doi:10.1061/(asce)0733-9445(2004)130:6(952).

[22] Jayas, B. S., & Hosain, M. U. (1988). Behaviour of Headed Studs in Composite Beams: Push-Out Tests. Canadian Journal of Civil Engineering, 15(2), 240–253. doi:10.1139/l88-032.

[23] Ghiami Azad, A. R. (2016). Fatigue behavior of post-installed shear connectors used to strengthen continuous non-composite steel bridge girders. PhD Thesis, The University of Texas at Austin, Austin, United States.

[24] Lowe, D., Das, R., & Clifton, C. (2014). Characterization of the Splitting Behavior of Steel-concrete Composite Beams with Shear Stud Connection. Procedia Materials Science, 3(August), 2174–2179. doi:10.1016/j.mspro.2014.06.352.

[25] Suwaed, A. S. H., He, J., & Vasdravellis, G. (2022). Experimental and Numerical Evaluation of a Welded Demountable Shear Connector through Horizontal Pushout Tests. Journal of Structural Engineering, 148(2), 1–13. doi:10.1061/(asce)st.1943-541x.0003269.

[26] Li, J., Liu, Z., Deng, J., & Chen, F. (2023). Bidirectional shear behavior of stud connectors in steel-concrete composite monorail track beams. Structural Concrete, 24(2), 2951–2964. doi:10.1002/suco.202200505.

[27] Ding, Y., Wang, X. D., Shen, M. H., Chung, K. F., Zhou, X. H., & Elghazouli, A. Y. (2024). Deformation characteristics of ductile large resistance shear connections for practical composite beams. Engineering Structures, 320. doi:10.1016/j.engstruct.2024.118838.

[28] Classen, M., & Gallwoszus, J. (2016). Concrete fatigue in composite dowels. Structural Concrete, 17(1), 63-73. doi:10.1002/suco.201400120.

[29] Al-Shuwaili, M. A., Palmeri, A., & Lombardo, M. T. (2018). A novel one-sided push-out test for shear connectors in composite beams. Proceedings 12th International Conference on Advances in Steel-Concrete Composite Structures - ASCCS 2018. doi:10.4995/asccs2018.2018.7063.

[30] Shen, M. H., & Chung, K. F. (2017). Structural Behaviour of Stud Shear Connections with Solid and Composite Slabs Under Co-Existing Shear and Tension Forces. Structures, 9, 79–90. doi:10.1016/j.istruc.2016.09.011.

[31] Ollgaard, J. G., Slutter, R. G., & Fisher, J. W. (1971). Shear Strength of Stud Connectors in Lightweight and Normal-Weight Concrete. Engineering Journal, 8(2), 55–64. doi:10.62913/engj.v8i2.160.

[32] Johnson, R. P., & Oehlers, D. J. (1987). The strength of stud shear connectors in composite beams. The Structural Engineer, 65, B2.

[33] Loh, H. Y., Uy, B., & Bradford, M. A. (2004). The effects of partial shear connection in the hogging moment regions of composite beams. Journal of Constructional Steel Research, 60(6), 897–919. doi:10.1016/j.jcsr.2003.10.007.

[34] Buttry, K. E. (1965). Behaviour of stud connectors in lightweight and normal-weight concrete. Master Thesis, University of Missouri, Columbia, United States.

[35] An, L., & Cederwall, K. (1996). Push-out Tests on Studs in High Strength and Normal Strength Concrete. Journal of Constructional Steel Research, 36(1), 15–29. doi:10.1016/0143-974X(94)00036-H.

[36] Xue, W., Ding, M., Wang, H., & Luo, Z. (2008). Static Behavior and Theoretical Model of Stud Shear Connectors. Journal of Bridge Engineering, 13(6), 623–634. doi:10.1061/(asce)1084-0702(2008)13:6(623).

[37] BS 5950-3.1:1990+A1:2010. (2010). Structural use of steelwork in building - Design in composite construction - Code of practice for design of simple and continuous composite beams. British Standards Institution (BSI), London, United Kingdom.

[38] Galjaard, H. C., Walraven, J. C., & Eligehausen, R. (2001, September). Static tests on various types of shear connectors for composite structures. 3rd International Symposium on Connections between Steel and Concrete. 27-29 September 2017, Stuttgart, Germany.

[39] Lam, D., & El-Lobody, E. (2005). Behavior of Headed Stud Shear Connectors in Composite Beam. Journal of Structural Engineering, 131(1), 96–107. doi:10.1061/(asce)0733-9445(2005)131:1(96).

[40] Shen, M. (2013). Structural behaviour of shear connection in composite structures under complex loading conditions. Ph.D. Thesis, Hong Kong Polytechnic University, Hung Hom, Hong Kong.

[41] Kumar, P., & Chaudhary, S. (2019). Effect of reinforcement detailing on performance of composite connections with headed studs. Engineering Structures, 179, 476–492. doi:10.1016/j.engstruct.2018.05.069.

[42] Lyons, J. C., Easterling, W. S., & Murray, T. M. (1994). Strength of headed shear studs (Vols. I & II, Report No. CE/VPI-ST 94/07). Virginia Polytechnic Institute and State University, Blacksburg, VA, United States.

[43] Lam, D. (2007). Capacities of headed stud shear connectors in composite steel beams with precast hollowcore slabs. Journal of Constructional Steel Research, 63(9), 1160–1174. doi:10.1016/j.jcsr.2006.11.012.